

The LLNL/UCLA HIGH GRADIENT INVERSE FREE ELECTRON LASER ACCELERATOR*

S.G. Anderson[†], G.G. Anderson, S.M. Betts, S.E. Fisher, D.J. Gibson,
A.M. Tremaine[‡], S.S. Wu, LLNL, Livermore, CA 94550, USA
J.T. Moody, P. Musumeci, UCLA, Los Angeles, CA 90095, USA

Abstract

We describe the Inverse Free Electron Laser (IFEL) accelerator currently under construction at LLNL in collaboration with UCLA. This project combines a strongly tapered undulator with a 10 Hz repetition rate, Ti:Sapphire laser to produce >200 MeV/m average accelerating gradient over the 50 cm long undulator. The project goal is to demonstrate IFEL accelerator technology that preserves the input beam quality and is well suited for future light source applications. We discuss the accelerator design focusing on issues associated with the use of 800 nm, 100 fs laser pulses. Three-dimensional simulations of the IFEL interaction are presented which guide the choice of laser and electron beam parameters. Finally, experimental plans and potential future developments are discussed.

INTRODUCTION

The IFEL is an advanced acceleration scheme that uses an undulator magnet to couple energy between laser radiation and electron forward motion. It is a promising candidate to demonstrate both high gradient and high quality acceleration within the 50 MeV to few GeV energy range and has the potential to be the acceleration mechanism in compact x- and γ -ray sources, or provide tabletop, GeV-class accelerators for academia and industry.

The IFEL acceleration mechanism was first proposed and analyzed in the 1980s [1, 2]. In first generation experiments, IFEL researchers demonstrated the IFEL mechanism as an effective pre-buncher [3], high beam trapping — 85% [4], and high gradient — 70 MeV/m [5], but never simultaneously, and no post IFEL acceleration beam quality measurements have been performed.

The second generation experiment described here combines 800 nm, Ti:Sapphire laser technology with the strongly tapered UCLA/Kurchatov IFEL undulator. This enables a compact accelerator with increased beam energy and energy gain using the same undulator as the previous CO₂ laser-based experiment [5]. Concurrently, the repetition rate is increased by several orders of magnitude, allowing multi-shot emittance measurements to determine the quality of the accelerated beam.

The multi-TW peak laser power required for high accelerating gradient is accomplished in Ti:Sapphire lasers by Chirped Pulse Amplification and subsequent compression to sub-picosecond pulse duration. In contrast to CO₂ laser experiments, these pulses can be short relative to the electron bunch duration and comparable to the amount of slippage in the undulator. We examine the consequences of using a short pulse laser to drive the IFEL in theoretical calculations and simulations, and use the results to determine the required parameters for the planned experiment.

We will use the LLNL 100 MeV electron linac and 1.6 cell photo-gun [6] to generate the 50 MeV beam required for injection into the IFEL accelerator. The linac consists of 5 independently powered and phased S-band 2.5 meter SLAC-type traveling wave sections. The flexibility of the rf system allows us to produce the beam energy required for IFEL injection as well as chirp the bunch for compression, used to increase the amount of charge accelerated by the short laser pulse. In the experiment described below, the injected beam interacts with a 500 mJ, 100 fs FWHM, 780 nm laser pulse in the 50 cm long undulator. The simulated energy of the captured beam at the end of the accelerator is 200 MeV. Downstream of the accelerator, a broadband spectrometer and quadrupole lattice are planned in order to measure the emittance, energy, and energy spread of the accelerated beam.

IFEL THEORY AND SIMULATION

The original IFEL analysis performed in Ref. [2] derives equations for the evolution of particle energy, $\gamma = E/mc^2$, and phase, ψ , for an electron acted upon by a sinusoidal undulator magnetic field on the beam axis, and a plane electromagnetic wave. In this experiment the laser beam is strongly focused (Rayleigh range much less than undulator length), and there is significant slippage of the electrons with respect to the laser duration (number of laser cycles and undulator periods is comparable). Thus, it is insufficient to model the laser field as a plane wave.

Instead, we assume a Gaussian spatial and temporal profile, giving the on-axis electric field,

$$\mathbf{E}_L = E_0 e^{-\frac{(kz - \omega t)^2}{(\omega\tau)^2}} \frac{w_0}{w(z)} \cos(kz - \omega t - \phi_G) \hat{\mathbf{x}}, \quad (1)$$

where E_0 is the peak electric field, k the laser wave number, $\omega = ck$, 2τ the e^{-2} intensity pulse duration, $w_0/w(z)$ the ratio of the minimum beam size to that at position z , and

* This work performed under the auspices of the U.S. Department of Energy by Lawrence Livermore National Laboratory under Contract DE-AC52-07NA27344.

[†] anderson131@llnl.gov

[‡] LLNL and UCLA affiliations

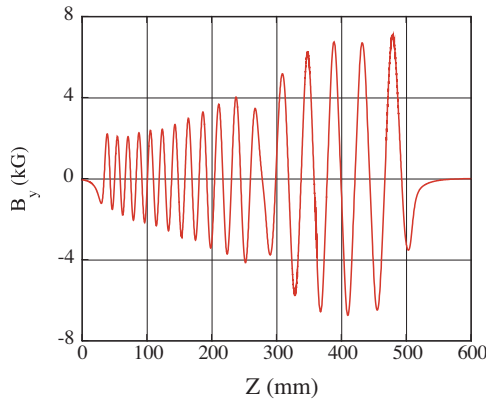


Figure 1: Measured vertical magnetic field component of the UCLA undulator.

ϕ_G is the Gouy phase, which shifts by π as the beam passes through the focus. Using a planar undulator magnetic field,

$$\mathbf{B}_w = B_0 \cos(k_w z) \hat{\mathbf{y}}, \quad (2)$$

and following the same analysis as Ref. [2], we find the accelerator equations,

$$\frac{d\gamma}{dz} = \frac{1}{2} \frac{k K_{L,eff} K_w}{\gamma} \text{JJ}_{eff} \sin \psi \quad (3)$$

$$\frac{d\psi}{dz} = k_w - k \frac{1 + K_w^2/2 + K_{L,eff}^2/2 + K_w K_{L,eff} \text{JJ}_{eff} \cos \psi}{2\gamma^2} - \frac{1}{z_r \left[1 + \left(\frac{z}{z_r} \right)^2 \right]}. \quad (4)$$

Here, $\psi = (k + k_w)z - \omega t - \phi_G$ is the relative phase, $K_w = \frac{eB_0}{mc k_w}$ the normalized undulator strength and,

$$K_{L,eff} = \frac{eE_0}{mc^2 k} \frac{w_0}{w(z)} e^{-\frac{(kz - \omega t)^2}{(\omega\tau)^2}} \quad (5)$$

is the normalized laser field strength. JJ_{eff} is the usual Bessel function term arising in planar geometries — see Ref. [2] — but in this case a function of $K_{L,eff}$, and $z_r = kw_0^2/2$ is the laser Rayleigh range.

These accelerator equations show that the IFEL dynamics are altered in two significant way for this experiment. Firstly, as studied by Musumeci [7], the Gouy phase shift — responsible for the last term in Eq. 4 — must be accounted for to maintain the resonant phase condition. In this experiment the phase shift is compensated using a longitudinal gap between magnets in the center of the undulator. The undulator therefore sets the Rayleigh range, $z_r = 3.5\text{cm}$, and the focusing parameters of the laser pulse. The undulator phase shift can be seen in the measured vertical field profile shown in Fig. 1

The second important change to Eqns. 3 and 4 is the dependence of $K_{L,eff}$ on the global values of z and t . Equation 5 is valid under the assumption that the Slowly Varying

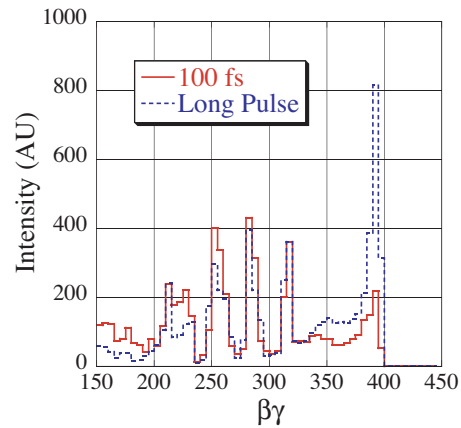


Figure 2: Normalized momentum spectrum exiting the undulator for 3 TW long laser pulse and 3 TW peak, 100 fs FWHM pulse.

Envelope Approximation (SVEA) holds, or in this case that $\omega\tau \gg 1$ and $kz_r \gg 1$.

To simulate the short pulse IFEL, it is clear that one must track separately each of the longitudinal slices of particles interacting with the laser pulse instead of choosing a representative ‘bucket’ of 2π phase extent. Further, to represent a realistic undulator, *i.e.*, that shown in Fig 1, and to include 3D effects, it is useful to step back from the accelerator equations and simulate particle motion using the Lorentz force law applied to the IFEL,

$$\frac{d\mathbf{p}}{dt} = e \left[(\mathbf{v} \times \mathbf{B}_w) + \mathbf{E}_L \left(1 - \frac{v_z}{c} \right) + \hat{\mathbf{z}} \left(\mathbf{v} \cdot \frac{\mathbf{E}_L}{c} \right) \right]. \quad (6)$$

In the simulation results that follow, particles are pushed through the IFEL interaction using measured field data for \mathbf{B}_w , and a Gaussian laser pulse — including off-axis phase and intensity variation.

In the simplest case, we examine the effect of a short laser pulse by comparing simulations of a 100 fs FWHM, 3 TW peak power laser, with a 3 TW laser with pulse length much longer than the interaction length in the 50 cm undulator. For this comparison the injected electron beam is mono-energetic with particles equally spaced in phase. The normalized momentum spectrum of the exiting beam is shown for both lasers in Fig. 2. In the long pulse case, each electron beam slice acts identically, as one expects, and we see a well defined captured bunch just below $\beta\gamma = 400$. In the short pulse case, there is a much narrower window of accelerated particles, however there are very few particles captured that exit the accelerator at full energy. While 3 TW is sufficient laser power when applied through the entire interaction, it is insufficient when using 100 fs, FWHM pulses, since all beam slices are below the capture threshold for some part of the interaction.

The result is that the peak laser power must be increased for short pulse IFEL to produce sufficient capture in the duration of the laser pulse. Simulations using a con-

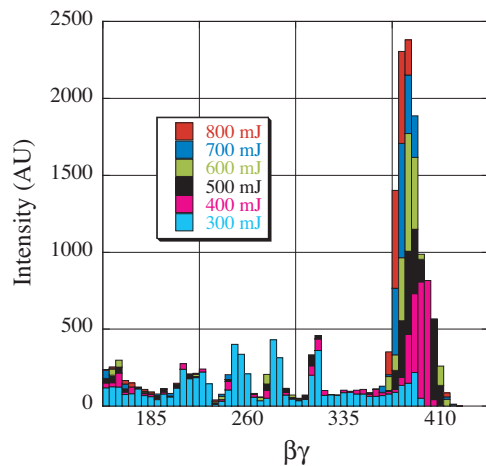


Figure 3: Simulated output spectra using 100 fs, 300 to 800 mJ laser pulses.

stant pulse duration but increasing laser energy have been performed, with the resulting output momentum spectra shown in Fig. 3. Here we see that 4-500 mJ of laser energy should produce a captured electron bunch, with increasing laser energy increasing the number of captured particles, but having a minimal effect on the energy of the captured bunch. Similarly, choosing 550 mJ of laser energy and scanning the pulse duration shows that there is a relatively broad optimum around 100 fs, FWHM, with the amount of captured charge falling off at 40 fs, and again above 150 fs.

EXPERIMENTAL SETUP

A Ti:Sapphire laser system capable of >500 mJ and <120 fs pulses was chosen for this experiment based on the simulations above and compatibility with the project budget. The system consists of a Er-doped fiber oscillator, stretcher, regenerative amplifier, and 4-pass amplifier producing 10 Hz, 25 mJ pulses. The beam is then split, sending 2 mJ to a low energy compressor and third harmonic generation stage. The resulting 260 nm, 100 μ J, 100 fs pulses drive the photoinjector, and can be temporally shaped using a pulse stacker, or sent directly to the cathode to produce electrons using the blow-out technique. The remaining 22 mJ laser pulses are sent through a delay line — used to synchronize the arrival of the laser and electrons at the undulator — to the main amplifier and subsequent vacuum compressor and transport line to the accelerator.

For these laser parameters and several ps electron beams, the above simulations indicate that the IFEL will capture ≈ 3.5 pC of charge per 100 Amps of beam current. Therefore, we have investigated the use of a chicane to compress a 125 pC electron beam generated using the blow-out technique and chirped running the final accelerator section at the rf zero crossing. Simulations using PARMELA and ELEGANT show that bunches as short as 100 fs are possible using this scheme. Feeding the electron beam phase space from ELEGANT into our IFEL simulation produces the out-

Advanced Concepts and Future Directions

Accel/Storage Rings 14: Advanced Concepts

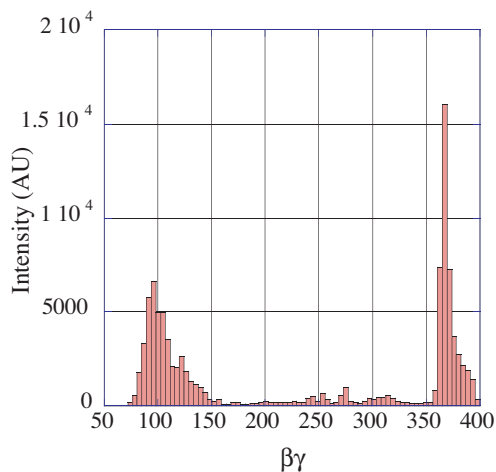


Figure 4: Start-to-end simulation of the output spectra using a 100 fs compressed electron bunch. Approximately 40% of the injected beam is captured.

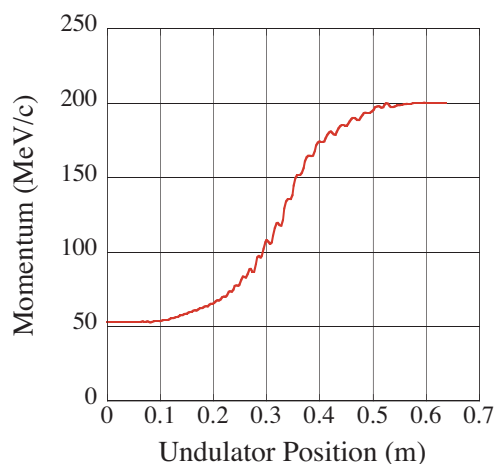


Figure 5: Momentum of captured particles versus undulator position. The laser and electron beams are focused at the center of the undulator, at $z = 32$ cm. The simulation predicts an average gradient approaching 300 MeV/m.

put spectrum and captured beam energy profile shown in Figures 4 and 5, respectively, giving 55 pC in the captured bunch accelerated from 50 to 200 MeV in the 50 cm undulator.

REFERENCES

- [1] R. Palmer, IEEE Trans. Nucl. Sci. **28** 3370 (1981).
- [2] E.D. Courant, C. Pellegrini, and W. Zakowicz, Phys. Rev. A **32** 2813 (1985).
- [3] Y. Liu, *et. al.*, Phys. Rev. Lett. **80** 4418 (1998).
- [4] W.D. Kimura, *et. al.*, Phys. Rev. Lett. **86** 4041 (2001).
- [5] P. Musumeci, *et. al.*, Phys. Rev. Lett. **94** 154801 (2005).
- [6] S.G. Anderson, *et. al.*, Proc. of PAC07, p. 1242 (2007).
- [7] P. Musumeci, Ph.D. Thesis, UCLA (2004).